This article has been accepted for publication in a future issue of this journal, but has not been fully edited. Content may change prior to final publication. Citation information: DOI 10.1109/TCSII.2016.2551547, IEEE Transactions on Circuits and Systems II: Express Briefs

Improving Load Range of Dual-Band Impedance Matching Networks using Load-Healing Concept

Mohammad A. Maktoomi, *Graduate Student Member, IEEE*, Mohammad S. Hashmi, *Member, IEEE*, Fadhel M. Ghannouchi, *Fellow*, *IEEE*

***Abstract*—A novel and very simple scheme to mend conventional dual-band impedance matching networks is presented. It involves the employment of a load modifying element (load-healer) so as to extend the range of frequency-dependent complex load that could be matched. Two simple load-healers incorporated in the conventional T-Network are used to illustrate the concept. The proposed scheme can be successfully applied in many situations where conventional matching networks are severely limited. Two prototypes operating concurrently at 1GHz and 2GHz are designed corresponding to the two types of the load-healer. They are implemented on FR4 substrate having dielectric constant of 4.6, substrate height of 1.5mm, and 35µm copper cladding. The prototypes exhibit good agreement between their EM simulated and measured results.**

***Index Terms*— Amplifier, dual-band, impedance matching, matching network, power divider.**

I. Introduction

With the unprecedented advancements in multi-band/multi-standard wireless communication systems, devices and systems that are capable of operating concurrently at multiple frequencies have gained huge research interest [1]. On the other hand, impedance matching network is the key component in most of the RF/microwave devices such as amplifiers, power dividers/couplers, antenna arrays, mixers and oscillators. They are also a very useful element in the design of RFID and energy harvesting circuits [2]-[3].

In most of the practical scenarios, especially, in case of amplifiers, the load impedance is complex as well as frequency-dependent [4]. Numerous dual-band designs have been reported in literature to meet this requirement [5]-[13].

However, conventional dual-band matching circuits have limited available range of load that could be matched. For implementation in microstrip technology, the limit of characteristic impedance that could normally be fabricated is 20Ω to 140Ω [8]. However, there always exists the load value that results into practically unrealizable values of the constituent elements of a particular matching topology. It is due to the fact that the load (to the matching network), $Z_L=R_1+jX_1$ @f_1 and $Z_L=R_2+jX_2$ @f_2 can take any value depending on the design frequencies, the biasing condition and the transistor being used. Table I lists some examples that cannot be realized using the conventional T-network [5]. It is apparent that for all the three cases, the matching network is practically unrealizable. It is due to one or more constituent elements having characteristic impedance that is beyond the limit of fabrication. In such scenario, one either switches to some other reported matching network topologies or uses multiple stages [6].

Therefore, for the first time, a novel and very simple technique for dual-band matching networks that we call **load-healing** is proposed in this paper. In a nutshell, the idea is to tune the load itself that the matching network effectively sees until a realizable design is obtained. This concept is illustrated in this paper using the conventional T-network, but the idea remains valid for other designs as well.

II. Proposed Scheme

The proposed dual-band impedance matching network scheme is illustrated in Fig.1. The task is to match a frequency-dependent complex load, $Z_L=R_1+jX_1$ @f_1 and $Z_L=R_2+jX_2$ @f_2 to a real source impedance, Z_0 (usually, =50Ω). A load-healing element is embedded between the conventional T-network and the load. In fact, the load-healer could be as complex as another T-network itself, but a fair requirement of the load-healer is to be as simplistic as possible. Therefore, two simple load-healers named as type-1, which is a simple transmission line (TL) section, and type-2, which is an open circuited stub, is used here to illustrate the whole idea. A short circuited stub is also feasible as load healer but at the cost of increased step of digging a via to the ground.

The overall working of the proposed network is as follows: The load-healing element modifies the load and transforms Z_L into another frequency dependent complex load Z_{Lx} ($=R_{1x}+jX_{1x}$ @f_1 and $=R_{2x}+jX_{2x}$ @f_2), which is a function of Z_x, θ_x, and $r=f_2/f_1$. Now, section A of the T-network transforms Z_{Lx} into an admittance, Y_{2n} which is related by complex conjugate relation at the two frequencies, that is $Y_{2n}\big|_{f_1} = Y_{2n}^*\big|_{f_2}$.

Manuscript received September 15, 2015, Revised on December 01, 2015, on January 27, 2016, and on March 09, 2016.

M. A. Maktoomi and M. S. Hashmi are with the CDRL, IIIT Delhi, New Delhi-110020, India and also with the iRadio Lab, University of Calgary, Calgary, AB T2N1N4, Canada (e-mails: {ayatullahm, mshashmi}@iiitd.ac.in).

F. M. Ghannouchi is with the iRadio Lab, University of Calgary, Calgary, AB T2N 1N4 (e-mail: fghannou@ucalgary.ca).

This article has been accepted for publication in a future issue of this journal, but has not been fully edited. Content may change prior to final publication. Citation information: DOI 10.1109/TCSII.2016.2551547, IEEE Transactions on Circuits and Systems II: Express Briefs

TABLE I
SOME CASES WHERE CONVENTIONAL T-TYPE NETWORK [5] CANNOT BE REALIZED

Case	Frequency (GHz)	$Z_L(\Omega)$	Nikravan's Design[5]			
			Z_a/θ_a	Z_b/θ_b		Z_c/θ_c
1	f_1=1 f_2= 2	10.272 +j11.866 11.061+j24.374	Z_a=**167.78Ω** θ_a =60°	Open Stub Z_b=**166.3Ω** θ_b=60°	Short stub Z_b =55.4Ω θ_b=120°	Z_c=76.64Ω θ_c=51.03°
2	f_1=1 f_2= 2.5	155.921-j27.021 130.383-j54.805	Z_a=73.09 Ω θ_a=51.53°	Open Stub Z_b=**838.2Ω** θ_b=102.86°	Short stub Z_b=**152.56Ω** θ_b=51.43°	Z_c=75.62Ω θ_c=45.42°
3	f_1=1.5 f_2= 2.5	86.547+j13.384 90.133+j21.835	Z_a=94.97 Ω θ_a=67.5°	Open Stub Z_b=**524.8Ω** θ_b=67.5°	Short stub Z_b=**217.39Ω** θ_b=135°	Z_c=121.68Ω θ_c=55.29°

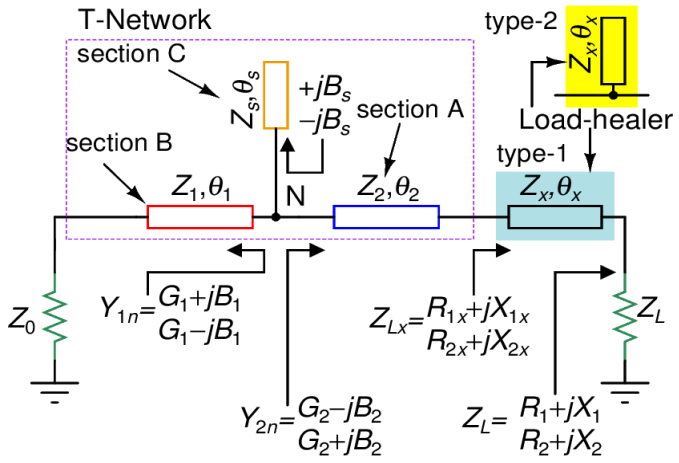

Fig. 1. Proposed matching scheme incorporating lead-healing element.

Similarly, section B is used to transform the source impedance, Z_0 into an admittance Y_{1n} such that $Y_{1n}\big|_{f_1} = Y_{1n}^*\big|_{f_2}$. To achieve complex conjugate matching, the real part of Y_{1n} is equated that to the real part of Y_{2n} and the remaining net imaginary part at the node N is cancelled by section C, which is a dual-band stub. Design equations of the proposed matching network are discussed in the next section.

III. ANALYSIS AND DESIGN

The design equations for the various elements of the proposed transformer are derived as follows.

A. The Load-Healer

Considering the type-1 load-healer first, Z_{Lx} is found by using the formula of input impedance of a loaded TL section:

$$Z_{Lx} = Z_x \frac{Z_L + jZ_x \tan\theta_x}{Z_x + jZ_L \tan\theta_x} \tag{1}$$

Now, rationalizing and separating the real and imaginary parts yields R_{1x} and X_{1x}:

$$R_{1x} = \frac{R_1 Z_x^2 \sec^2\theta_x}{(Z_x - X_1\tan\theta_x)^2 + (R_1\tan\theta_x)^2} \tag{2}$$

$$X_{1x} = Z_x \frac{(X_1 + Z_x\tan\theta_x)(Z_x - X_1\tan\theta_x) - R_1^2\tan\theta_x}{(Z_x - X_1\tan\theta_x)^2 + (R_1\tan\theta_x)^2} \tag{3}$$

Since, electrical length is proportional to frequency [1], therefore, θ_x defined at f_1 becomes $r\theta_x$ at f_2. Thus, R_{2x} and X_{2x} are given as follows:

$$R_{2x} = \frac{R_2 Z_x^2 \sec^2 r\theta_x}{(Z_x - X_2\tan r\theta_x)^2 + (R_2\tan r\theta_x)^2} \tag{4}$$

$$X_{2x} = Z_x \frac{(X_2 + Z_x\tan r\theta_x)(Z_x - X_2\tan r\theta_x) - R_2^2\tan r\theta_x}{(Z_x - X_2\tan r\theta_x)^2 + (R_2\tan r\theta_x)^2}. \tag{5}$$

It is very simple thing to see from (2) - (5) that:

$$\lim_{\theta_x\to 0} Z_{Lx} = Z_L. \tag{6}$$

And, thus, strength of the proposed scheme is clearly evident: it can be used for all those impedances normally handled by the conventional T-type matching network in addition to what cannot be handled by the same.

Now, considering the type-2 load-healer, Z_{Lx} is given by the following expression:

$$Z_{Lx} = Z_L \,||\, -jZ_x\cot\theta_x = \frac{-jZ_xZ_L\cot\theta_x}{Z_L - jZ_x\cot\theta_x} \tag{7}$$

Following the same procedure as is opted for type-1 load-healer, the following expressions are obtained in this case:

$$R_{1x} = \frac{R_1 Z_x^2\cot^2\theta_x}{R_1^2 + (X_1 - Z_x\cot\theta_x)^2} \tag{8}$$

$$X_{1x} = \frac{Z_x\cot\theta_x\left[R_1^2 + X_1(X_1 - Z_x\cot\theta_x)\right]}{R_1^2 + (X_1 - Z_x\cot\theta_x)^2} \tag{9}$$

$$R_{2x} = \frac{R_2 Z_x^2\cot^2 r\theta_x}{R_2^2 + (X_2 - Z_x\cot r\theta_x)^2} \tag{10}$$

$$X_{2x} = \frac{Z_x\cot r\theta_x\left[R_2^2 + X_2(X_2 - Z_x\cot r\theta_x)\right]}{R_2^2 + (X_2 - Z_x\cot r\theta_x)^2} \tag{11}$$

Condition given by (6) also holds true for the type-2 load-healer.

B. Design of Section A

The function of section is to transform Z_{Lx} into an admittance Y_{2n}, such that $Y_{2n}|_{f1} = Y_{2n}^*|_{f2}$. And, therefore, this section is designed using the following equations [13]:

$$Z_2 = \sqrt{R_{1x}R_{2x} + X_{1x}X_{2x} + \frac{X_{1x}+X_{2x}}{R_{2x}-R_{1x}}(R_{1x}X_{2x} - R_{2x}X_{1x})} \tag{12}$$

This article has been accepted for publication in a future issue of this journal, but has not been fully edited. Content may change prior to final publication. Citation information: DOI 10.1109/TCSII.2016.2551547, IEEE Transactions on Circuits and Systems II: Express Briefs

$$\theta_2 = \frac{p\pi + \arctan\left(\dfrac{Z_{1x}(R_{1x}-R_{2x})}{R_{1x}X_{2x}-R_{2x}X_{1x}}\right)}{1+r}, p \in \text{integer}. \quad (13)$$

With the section A designed using (12) - (13), the value of G_2 and B_2 are given by the following relations [9]:

$$G_2 = \frac{a}{a^2+b^2} \quad (14)$$

$$B_2 = \frac{b}{a^2+b^2} \quad (15)$$

Where, a and b are given by (16) - (17):

$$a = \frac{R_{1x}Z_2^2[1+\tan^2\theta_2]}{Z_2^2 - 2Z_2X_{1x}\tan\theta_2 + (R_{1x}^2+X_{1x}^2)\tan^2\theta_2} \quad (16)$$

$$b = \frac{(Z_2^2 - R_{1x}^2 - X_{x1}^2)Z_2\tan\theta_2 + Z_2^2X_{1x}(1-\tan^2\theta_2)}{Z_2^2 - 2Z_2X_{1x}\tan\theta_2 + (R_{1x}^2+X_{1x}^2)\tan^2\theta_2} \quad (17)$$

C. Design of Section B

Applying formula of input impedance, Y_{1n} can be expressed as G_1+jB_1 with G_1 and B_1 given by:

$$G_1 = \frac{Z_0\left(1+\tan^2\theta_1\right)}{Z_0^2 + Z_1^2\tan^2\theta_1} \quad (18)$$

$$B_1 = \frac{\left(Z_0^2 - Z_1^2\right)\tan\theta_1}{Z_1\left(Z_0^2 + Z_1^2\tan^2\theta_1\right)} \quad (19)$$

It is apparent from (18)-(19) that if θ_1 is replaced by π- θ_1, then G_1 remains the same, whereas B_1 just changes its sign. And, therefore, θ_1 if selected as given by (20), implies $Y_{1n}|_{f1} = Y_{1n}^*|_{f2}$, that is, if $Y_{1n}=G_1+jB_1$ @f_1, then $Y_{1n}=G_1 - jB_1$ @f_2 and vice-versa:

$$\theta_1 = \frac{q\pi}{1+r}, q \in \text{integer}. \quad (20)$$

Setting $G_1=G_2$, leads to the expression of Z_1:

$$Z_1 = \frac{1}{\tan\theta_1}\sqrt{\frac{Z_0(1+\tan^2\theta_1)}{G_2} - Z_0^2} \quad (21)$$

D. Design of Section C

Having designed the section A and section B, the last step is to cancel the left-over imaginary parts of Y_{1n} and Y_{2n} at the junction N. The net sum of imaginary parts are $+(B_1-B_2)$ @f_1 and $-(B_1-B_2)$ @f_2. Since, admittance sums at a junction, the task is to synthesize an admittance that is equal to $-(B_1-B_2)$ @f_1 and $+(B_1-B_2)$ @f_2. There are three simple options to synthesize these admittances as shown in Fig. 2. Noting that θ_s defined at f_1 becomes $r\theta_s$ at f_2, an open stub needs to satisfy the following equations:

$$(B_2 - B_1) = Y_s|_{f_1} = \tan\theta_s / Z_s \quad (22)$$

$$-(B_2 - B_1) = Y_s|_{f_2} = \tan r\theta_s / Z_s \quad (23)$$

Solving (22) and (23) simultaneously gives the following design equations:

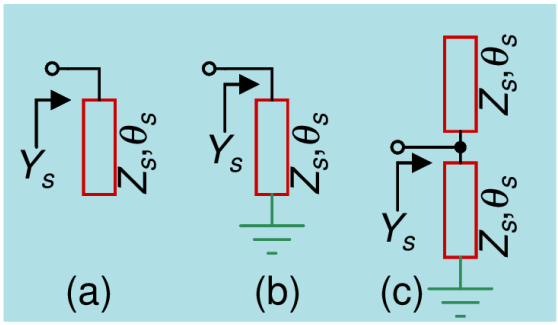

Fig. 2. (a) Dual-band stubs to be used as section C (a) open, (b) short , and (c) open-short combination.

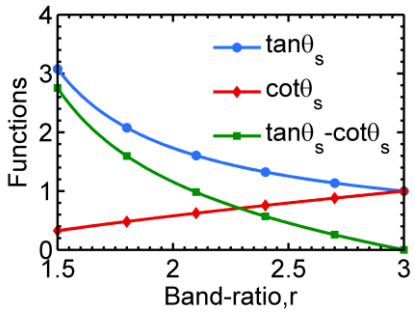

Fig. 3. Numerators of stub design equations against the band-ratio.

$$Z_s = \tan\theta_s / (B_2 - B_1) \quad (24)$$

$$\theta_s = \frac{m\pi}{1+r}, m \in \text{integer}. \quad (25)$$

Design equations for a short stub (Fig. 2(b)) remains the same except that $-\cot\theta_s$ be used in (24), instead of $\tan\theta_s$ [9]. Moreover, if an open-short stub combination (Fig. 2(c)) is to be used then the designs equations are as follows:

$$Z_s = (\tan\theta_s - \cot\theta_s) / (B_2 - B_1) \quad (26)$$

Although, intention here only is to highlight the load-healing concept employed in dual-band matching, but it is interesting to consider the open-short combination a little further since it has not been discussed in [5]. For this purpose, three functions, namely the numerators of the design equations of the three stubs, $\tan\theta_s$, $\cot\theta_s$, and $\tan\theta_s - \cot\theta_s$, are plotted in Fig.3. It is apparent that for r>2.3, $\tan\theta_s - \cot\theta_s$ is lesser than the other two functions. An implication of this fact is that the open-short combination may yield a realizable value of Z_s, while the other two may not. For example, if r =2.7, and B_2-B_1=0.0025, then the required value of Z_s are 454.5Ω, 352Ω and 102.5Ω, respectively, for the open, short and open-short combination. And, thus the advantage of using the open-short stub type should be evident.

E. Design Procedure

The flowchart of design procedure is illustrated in Fig. 4. The design begins with assuming a suitable value of Z_x and θ_x. Ideally, θ_x should be selected as small as possible and, Z_x must lie within the range of 20Ω to 140Ω. Moreover, during the design cycle, characteristics impedance of each of the TL section of T-network must be ensured within the fabrication limit, otherwise one needs to change Z_x or θ_x or both.

This article has been accepted for publication in a future issue of this journal, but has not been fully edited. Content may change prior to final publication. Citation information: DOI 10.1109/TCSII.2016.2551547, IEEE Transactions on Circuits and Systems II: Express Briefs

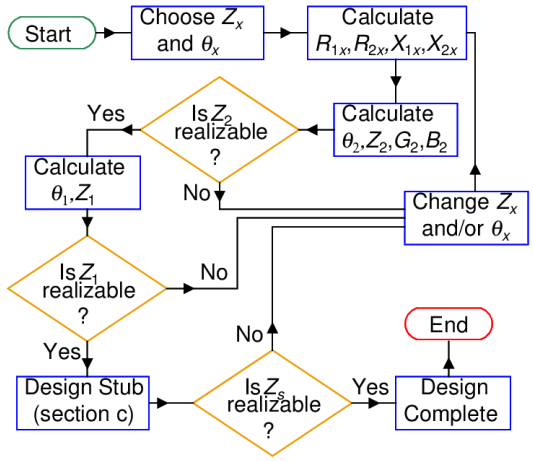

Fig. 4. Flowchart illustrating the design procedure.

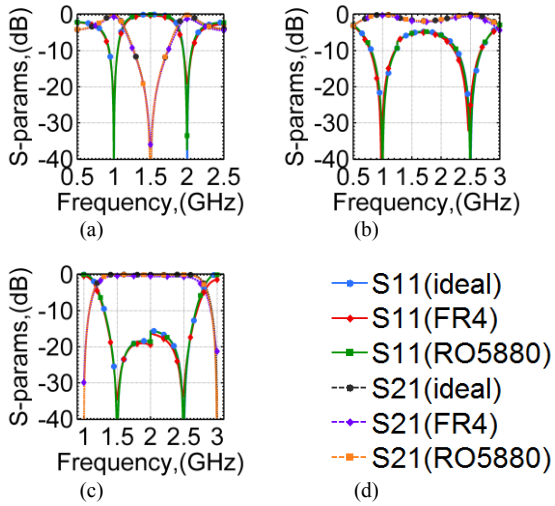

Fig. 5. Simulated return and insertion loss corresponding to the Table II designs (a) Case 1(b) Case 2 (c) Case 3, and (d) legend.

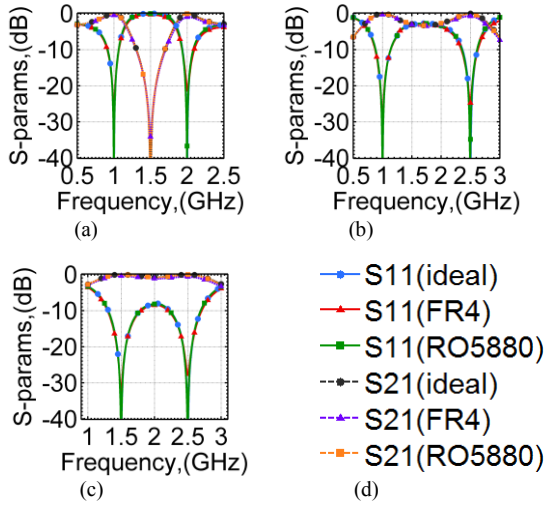

Fig. 6. Simulated return and insertion loss corresponding to the Table III designs (a) Case 1(b) Case 2 (c) Case 3, and (d) legend.

While designing section C, all the three types of stub are designed to find the most suitable one, unless there is design restriction on using short stub. The integers, p, q, and m are usually selected either equal to 1 or 2 to achieve compact size and to ensure positive value of various TL sections [9].

TABLE II
PROPOSED NETWORK (TYPE-1) PARAMETERS FOR CASES OF TABLE I

Case	Z_x/θ_x	Z_2/θ_2	Z_1/θ_1	Z_s/θ_s
1	Z_x=40Ω θ_x =10°	Z_2=49.3Ω θ_2=37.03°	Z_1 =105.9Ω θ_1=60°	Z_s=113.8Ω θ_s=60° Open Stub
2	Z_x=60Ω θ_x =5°	Z_2=64.2Ω θ_2=41.26°	Z_1 =69.52Ω θ_1=51.43°	Z_s=88.33Ω θ_s=51.43° Short Stub
3	Z_x=60Ω θ_x =30°	Z_2=46.5Ω θ_2=54.3°	Z_1 =40.48Ω θ_1=67.5°	Z_s=53.84Ω θ_s=135° Open Stub

TABLE III
PROPOSED NETWORK (TYPE-2) PARAMETERS FOR CASES OF TABLE I

Case	Z_x/θ_x	Z_2/θ_2	Z_1/θ_1	Z_s/θ_s
1	Z_x=30Ω θ_x =5°	Z_2=41.2Ω θ_2=42.22°	Z_1 =87.4Ω θ_1=60°	Z_s=100.8Ω θ_s=60° Open Stub
2	Z_x=80Ω θ_x =4°	Z_2=45.77Ω θ_2=45.88°	Z_1 =64.87Ω θ_1=51.43°	Z_s=42.48Ω θ_s=51.43° Short Stub
3	Z_x=120Ω θ_x =4°	Z_2=99.25Ω θ_2=46.5°	Z_1 =92.9Ω θ_1=135°	Z_s=84.4Ω θ_s=67.5° Short Stub

TABLE IV
DESIGN PARAMETERS OF PROTOTYPE WITH TYPE-1 LOAD-HEALER

Params.	Z_x/θ_x	Z_2/θ_2	Z_1/θ_1	Z_s/θ_s
Ideal	Z_x=40Ω θ_x =10°	Z_2=50.7Ω θ_2=39.8°	Z_1 =45.4Ω θ_1=60°	Z_s=105.3Ω θ_s=120° Open Stub
W/L(mm) Calc.	W=3.98 L =4.41	W=2.71 L =17.89	W=3.26 L =26.73	W=0.51 L =57.21
W/L(mm) Optm.	W=3.62 L =4.35	W=2.91 L =17.65	W=3.74 L =25.98	W=0.48 L =56.85

TABLE V
DESIGN PARAMETERS OF PROTOTYPE WITH TYPE-2 LOAD-HEALER

Params.	Z_x/θ_x	Z_2/θ_2	Z_1/θ_1	Z_s/θ_s
Ideal	Z_x=90Ω θ_x =10°	Z_2=49.37Ω θ_2=46.45°	Z_1 =45Ω θ_1=60°	Z_s=99Ω θ_s=120° Open Stub
W/L(mm) Calc.	W=0.80 L =4.72	W=2.83 L =20.83	W=3.30 L =26.72	W=0.61 L =56.93
W/L(mm) Optm.	W=0.73 L =4.18	W=3.00 L =21.34	W=3.77 L =27.92	W=0.51 L =58.84

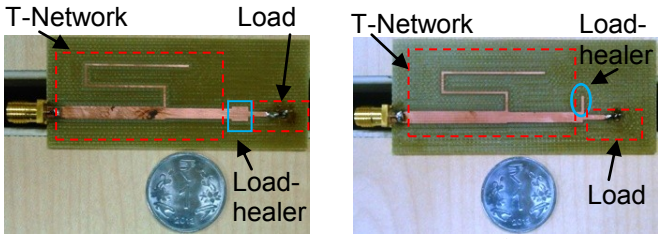

Fig. 7. Fabricated prototypes with (a) type-1 and (b) type-2 load-healers.

IV. DESIGN EXAMPLES, PROTOTYPING, AND MEASUREMENT

The same design cases listed in Table I that cannot be realized using the conventional T-network are chosen as the design examples. The corresponding design parameters of the proposed technique are listed in Table II with type-1 load-

This article has been accepted for publication in a future issue of this journal, but has not been fully edited. Content may change prior to final publication. Citation information: DOI 10.1109/TCSII.2016.2551547, IEEE Transactions on Circuits and Systems II: Express Briefs

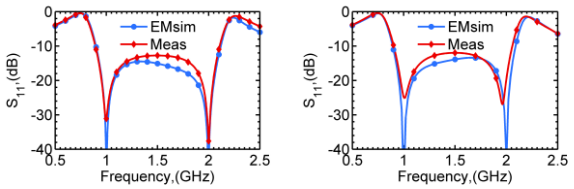

Fig. 8. EM simulated and the measured return loss of the prototype with (a) type-1 load-healer and (b) type-2 load-healer.

healer and in Table III with type-2 load- healer. It is apparent that none of parameters are beyond the impedance limit of 20Ω to 140Ω. Moreover, it is interesting to observe how addition of very small length of TL section turns otherwise unrealizable design into realizable ones. It must be noted that since Z_x and θ_x are free variables, examples in Table II/Table III show only one possible value for each case. Figs. 5 and 6 show the return and insertion losses of the design cases listed in Tables II and III, respectively. The simulation results have been obtained using ideal transmission lines as well as their implementation in FR4 (ϵ_r=4.6, height=1.5mm, copper cladding =35µm, and loss-tangent=0.02) and in Roger's RO5880® (ϵ_r=2.2, height=1.5mm, copper cladding =35µm, and loss-tangent=0.0009) microstrip substrates. The corresponding dimensions can easily be calculated using any line calculator software, such as ADS LineCalc®. A good matching and insertion loss performance is evident from these plots. Moreover, since RO5880® is a very low loss and more frequency stable material, therefore, performance obtained using this substrate is better than the corresponding results obtained using FR4.

In general, the load-healer will also modify the band-width, but since the load itself is frequency dependent so defining band-width in such case is a vague idea as intuitively explained in [12].

Two prototypes for Z_L= 92.971-*j*15.784Ω @ 1GHz and Z_L= 78.816-*j*21.529Ω @ 2GHz are designed corresponding to the two types of the load-healer. The frequency dependent load is a TL section in series with a 100Ω resistor. Their calculated design parameters are given in Table IV and Table V for the two types of the load-healers. This designs are implemented on FR4 substrate (ϵ_r = 4.6, height = 1.5mm, copper = 35µm) as shown in Fig. 7. The final designs need a little optimization, for example, to take junction discontinuity into account. Table IV and Table V also provides the calculated and optimized design dimensions (all dimensions are in mm) for various parameters (params.). The corresponding electromagnetic simulated (EMsim) and measured (Meas) return losses depicted in Fig. 8 are in good agreement of each other.

V. Discussion

The limited load-range of the design reported in [5] is partly due to the fact that section-A comes directly after the load. The load being complex and distinct at the two frequencies, puts a heavy burden on the section-A for transforming the same to a complex conjugate relation. The same limitation is also apparent in the designs of [2], [12], and [13] and in Ref. [2] of [3]. Therefore, the technique presented here can also be extended them. Moreover, Y_{in} in Fig. 1 of [11] must be equal to Y_0 (=1/Z_0), no such restriction is present in the proposed design due to the presence of Section B, which provides additional flexibility while handling frequency dependent complex loads.

VI. Conclusion

A novel concept of dual-band impedance matching incorporating load-healing has been introduced in this paper. An example circuit of conventional T-type network was analyzed in presence of two simple types of load-healers. Type-1 load healer adds (although most often very little) to the total length of the network, but may be preferable in cases where the type-2 load-healer would be difficult to incorporate during the layout. It is demonstrated through a number of examples that an otherwise unrealizable dual-band matching network could easily be realized by incorporating load-healers. The presented scheme is generic in nature and could potentially be applied in other conventional impedance matching networks as well. Moreover, a combination of type-1 and type-2 load-healers may also be a nice candidate but at cost of increased number of free variables and complexity.

References

[1] K. Rawat, M. S. Hashmi, and F. M. Ghannouchi, "Dual-band RF circuits and components for multi-standard software defined radios," *IEEE Circuits Syst. Mag.*, vol. 12, no. 1, pp. 12–32, Feb. 2012.

[2] Z. Liu, Z. Zhong, and Y.-X. Guo, "Enhanced dual-band ambient rf energy harvesting with ultra-wide power range," *IEEE Microw. Wireless Compon. Lett*., vol. 25, no. 9, pp. 630–632, Sept. 2015.

[3] Y. Wu, L. Jiao and Y. Liu, "Comments on "novel dual-band matching network for effective design of concurrent dual-band power amplifiers"," *IEEE Trans. Circuits Syst. I, Reg. Papers*, vol. 62, no. 9, pp. 2361–2361, Aug. 2015.

[4] G. Lee, J. Jung, and J.-I. Song, "A multiband power amplifier with a reconfigurable output-matching network for 10-MHz BW LTE mobile phone applications," *IEEE Trans. Circuits Syst. II, Exp. Briefs*, vol. 62, no. 6, pp. 558–562, June 2015.

[5] M. A. Nikravan and Z. Atlasbaf, "T-section dual-band impedance transformer for frequency-dependent complex impedance loads", *IET E. Letters*, vol.47, no.9, pp.551–553, Apr. 2011.

[6] K. Rawat and F. M. Ghannouchi, "Dual-band matching technique based on dual-characteristic impedance transformers for dual-band power amplifiers design," *IET Microwaves, Antennas & Propagation*, vol. 5, No. 14, pp.1720–1729, Nov. 2011.

[7] N. Nallam and S. Chatterjee, "Multi-band frequency transformations, matching networks and amplifiers," *IEEE Trans. Circuits Syst. I, Reg. Papers*, vol. 60, no. 6, pp. 1635–1647, Jun. 2013

[8] M.-L. Chuang, "Analytical design of dual-band impedance transformer with additional transmission zero," *IET Microwaves, Antennas & Propagation*, vol. 8, No. 13, pp.1120–1126, Oct. 2014.

[9] M. A. Maktoomi, M.S. Hashmi, and F. M. Ghannouchi, "A T-section dual-band matching network for frequency-dependent complex loads incorporating coupled line with dc-block property suitable for dual-band transistor amplifiers," *Prog. Electromagn. Res.* C (*PIER C*), vol. 54, pp. 75–84, 2014.

[10] S. C. Dutta Roy, "Characteristics of single- and multiple-frequency impedance matching networks," *IEEE Trans. Circuits Syst. II, Exp. Briefs*, vol. 62, no. 3, pp. 222–225, Mar. 2015.

[11] O. Manoochehri, A. Asoodeh, and K. Forooraghi, "Pi -model dual-band impedance transformer for unequal complex impedance loads," *IEEE Microw. Wireless Compon. Lett.*, vol.25, no.4, pp.238–240, Apr. 2015.

[12] M. A. Maktoomi, M. S. Hashmi, and V. Panwar, "A dual-frequency matching network for FDCLs using dual-band λ/4-lines," *Prog. Electromagn. Res.-L (PIER L)*, vol. 52, pp. 23–30,2015.

[13] X. Liu, Y. Liu, S. Li, F. Wu, and Y. Wu, "A three-section dual-band transformer for frequency-dependent complex load impedance", *IEEE Microw. Wireless Compon. Lett.*, vol. 19, no. 10, pp. 611–613, Oct. 2009.